Thin Solid Films 571 (2014) 302–307

Contents lists available at ScienceDirect

Thin Solid Films

journal homepage: www.elsevier.com/locate/tsf

Ductile film delamination from compliant substrates using hard overlayers

M.J. Cordill [a,*], V.M. Marx [b], C. Kirchlechner [b]

[a] Erich Schmid Institute of Materials Science, Austrian Academy of Sciences, Austria
[b] Max-Plank-Insitut für Eisenforschung GmbH, Düsseldorf, Germany

ARTICLE INFO

Available online 12 March 2014

Keywords:
Thin films
Adhesion
Polymer substrates
Stressed overlayers
Fragmentation testing

ABSTRACT

Flexible electronic devices call for copper and gold metal films to adhere well to polymer substrates. Measuring the interfacial adhesion of these material systems is often challenging, requiring the formulation of different techniques and models. Presented here is a strategy to induce well defined areas of delamination to measure the adhesion of copper films on polyimide substrates. The technique utilizes a stressed overlayer and tensile straining to cause buckle formation. The described method allows one to examine the effects of thin adhesion layers used to improve the adhesion of flexible systems.

© 2014 The Authors. Published by Elsevier B.V. This is an open access article under the CC BY-NC-ND license (http://creativecommons.org/licenses/by-nc-nd/3.0/).

1. Introduction

With the emergence of flexible sensors [1,2] and printable electronics [3–5], there becomes a need to determine the electrical and mechanical properties of metal and ceramic films on polymer substrates. One of the most important mechanical properties is the adhesion of metal lines and ceramic transistors to the polymer substrate [6,7]. These components must adhere well to the substrate in order to operate throughout a range of tensile, bending, and compressive strains that the device will be subjected to during use. Unfortunately, measuring the interfacial adhesion strength is difficult when using thin polymer substrates (between 12 μm and 100 μm thick) as residual stresses in deposited metal films can be large enough to cause macroscopic bending of the film–substrate system.

Techniques used to measure the adhesion energy of thin films on rigid substrates cannot always be utilized on compliant polymer substrates. For example, indentation induced delamination is hindered by the soft substrate [8,9], stress overlayers will macroscopically bend the sample [10,11], and four point bending requires extensive sample preparation and a large number of samples for good statistics [12,13]. More related to films on polymer substrates, a variety of studies have be performed [14–17] to measure the adhesion energy using a combination of techniques. However, most of these techniques are based on the fragmentation test. With fragmentation testing, films on polymer substrates are strained in tension until the film delaminates in the form of buckles which occur between the crack fragments. One available adhesion method uses the buckle dimensions in a thermodynamic based model to calculate the adhesion energy [18]. Thus far, the interfacial adhesion energy of Cr–polyimide (PI) [18], Cr–Polyethylene terephthalate (PET) [19], and Ti–PI [20,21] interfaces has been measured with this technique.

The difficulty arises when applying the same technique to more ductile film systems, such as Cu and Au, both candidate materials for current carrying elements in flexible devices and sensors. As shown by several groups [22–25], Cu films on polymer substrates deform plastically when strained in tension, leading to no delamination. The ductile films deform first via localized thinning or necking (necks) of the film, similar to necking of bulk ductile materials strained in tension. With further straining, the necks can become a crack that travels through the entire film to the film–substrate interface. Fig. 1 illustrates the difference between a neck and a crack. The combination of a stressed overlayer and tensile straining can force cracks through the ductile layer to the interface allowing for delamination to occur between crack fragments. This technique will be demonstrated on a Cu film with a Ti adhesion layer using a Cr stressed overlayer. The Cordill model [18] for adhesion is used to calculate the adhesion energy of the Ti–PI interface with an overlying ductile Cu film.

2. Materials/experimental

A 200 nm thick film of Cu was deposited onto 50 μm thick UPILEX brand PI substrates using e-beam evaporation. A Ti 30 nm interlayer was deposited between the Cu and PI to increase the adhesion of the interface. A similar film system was made with an additional 200 nm Cr film deposited on top of the Cu film to act as a stressed overlayer. For readability, the two film systems will be named according to their film materials, such as CuTi for the 200 nm Cu/30 nm Ti film system and CrCuTi for the 200 nm Cr/200 nm Cu/30 nm Ti film system. Initially, the Cr film had a columnar grain structure with grain size of about 20 nm and the Cu film had an average grain size of about 1 μm measured

* Corresponding author.

http://dx.doi.org/10.1016/j.tsf.2014.02.093
0040-6090/© 2014 The Authors. Published by Elsevier B.V. This is an open access article under the CC BY-NC-ND license (http://creativecommons.org/licenses/by-nc-nd/3.0/).

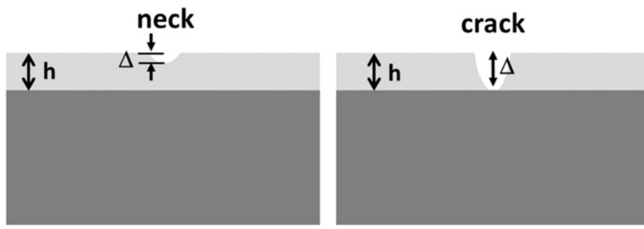

Fig. 1. Schematic diagram illustrating the difference between a locally thinned region (neck) and a crack that can form when a ductile film on a polymer substrate is strained. The depth of the deformation site is used to determine the character of the site, i.e. a neck or a crack.

from cross-sectional and plane-view transmission electron micrographs. The residual stresses of both film materials and systems were measured using X-ray diffraction and the $\sin^2\psi$ technique [26]. In the CrCuTi system, the Cr film had a tensile residual stress of 850 MPa and the Cu film a tensile residual stress of 200 MPa. The Cu film in the CuTi film system had a similar tensile residual stress of 250 MPa. The Ti layer could not be measured in either film system and its residual stress is unknown.

The evolution of stress in the CrCuTi film was measured in situ based on the $\sin^2\psi$ method using the KMC-II beam line at the Berliner Elektronenspeicherring-Gesellschaft für Synchrotronstrahlung (BESSY II) in Berlin, Germany [27]. The 300 μm sized monochromatic 7 keV beam was used to measure the lattice strains based on the Cu(111) and Cr(110) reflections at four different ψ angles. As a detector, a Vantec 2000 (Bruker AXS, Germany) with 5 s of exposure time was utilized. The lattice strains were used to derive the stresses parallel and perpendicular to the straining direction using the X-ray elastic constants for $1/2S_2$ of Cu(111) and Cr(110) calculated based on the Hill model [28]. A value of 0.7912 for the (111) Cu peak assuming the film was untextured and 0.4436 for the (110) Cr peak. The samples with a gauge length of 23 mm were continuously strained with an Anton Paar TS600® at a displacement rate of 2 μm/s to a maximum prescribed strain with a 5 minute hold before unloading to zero force at the same displacement rate. By this approach, the film stresses during fracture or yielding (parallel direction) and buckle formation (perpendicular direction) were evaluated. The stresses were correlated to the compound stress–strain curves of the film and substrate measured via the strain gauge and load cell of the TS600.

Both film systems (CuTi and CrCuTi) were strained in situ inside the scanning electron microscope (SEM). In situ straining inside the SEM was performed using a Kammrath and Weiss straining device. The samples had dimensions of 45 mm by 9 mm and an initial gauge length of approximately 22 mm was employed. Experiments inside the SEM were carried out by increasing the displacement in a stepwise fashion and an image taken at every step to correlate to the strain. In order to observe the initial fracture strain, small straining steps (50 μm) were utilized until cracking was observed. After cracking had initiated in the film, the straining steps were increased to 100 μm until buckling occurred (for the CrCuTi sample only) and then 200 μm steps until the prescribed maximum strain was reached. A 10 μm/s displacement rate was utilized for each straining step. From the SEM images, the initial fracture strain and buckling strain were determined as well as the crack and buckle spacing evolution using the line intercept method and Image J [29].

Additionally, the CuTi film was strained in situ under the atomic force microscope (AFM) [25,30–33] to better observe the surface deformation (necking) and crack formation as a function of strain. For this, a miniaturized screw-driven tensile stage was utilized with a 25 μm × 25 μm scan size at 1 Hz and a 512 dpi resolution. Using three surface profiles from each AFM image the spacing between deformation sites (necks and cracks) was measured. When a neck or crack is present in the surface profile they are indicated by a sharp decrease from the surface level as illustrated in Fig. 2. The criterion to distinguish between a neck and a crack is based on brittle film cracking and the measurable depth, Δ, of the crack or neck and the film thickness, h (see Fig. 1). The depth of the deformation site was determined with the AFM surface profile data and subtracting the lowest point of the deformation from all data points 250 nm on each side in order to get an average depth. A neck has been defined as having a $\Delta/h < 0.15$ and $\Delta/h > 0.15$ defines a through thickness crack [25,30]. Using Δ/h ratio, each deformation site can be described as a neck or a crack. An example of the method is shown in Fig. 2 for the CuTi film strained to 9.8%. In the AFM height image and surface profile the deformation sites are labeled as a crack (black arrows) or a neck (white or gray arrows). At each straining step the crack density and surface deformation density which included both cracks and necks was measured using the line-intercept method and the above criterion. For more information on the criterion and method see References [25,30]. Only the in situ AFM images were used to determine the crack and surface deformation densities of the CuTi film.

The AFM was also employed to image and measure the resulting buckles of CrCuTi film after straining. The buckle heights, δ, and half buckle widths, b, were used to calculate the adhesion energy of the failing Ti–PI interface using the model developed by Cordill et al. [18]. These values are plotted as $(\delta/h)^{1/2}$ as a function of (b/h) according to the relation

$$(\delta/h)^{1/2} = (2\alpha)^{1/4}(b/h)\left[1+\sqrt{1+(3/4)\alpha(b/h)^4}\right]^{-1/4} \quad (1)$$

where α is a fitting parameter. In Ref. [18] the development of Eq. (1) and further discussion of the method can be found. Additionally, the

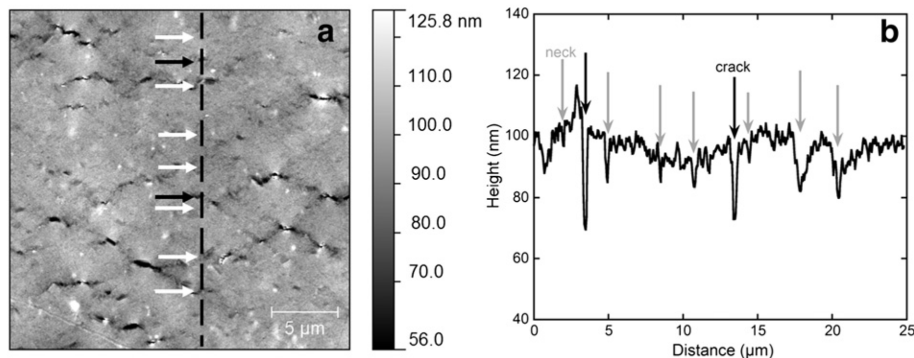

Fig. 2. (a) AFM height image of the CuTi film at 9.8% strain with the surface profile (dashed line) shown in (b) demonstrating how to determine if a surface deformation site is a neck or a crack. Cracks are indicated with black arrows and necks with white (a) or gray (b) arrows.

2D model of Cordill et al. [18] was modeled and compared to a 3D model [34]. The adhesion energy, Γ, is calculated with knowledge of the α parameter, the film thickness, h, and the modified elastic modulus, E', using

$$\alpha = \frac{4\Gamma}{hE'}\left(\frac{2}{\pi}\right)^4. \quad (2)$$

In Eq. (2), the E' ($E' = E / (1 - \nu^2)$) was weighted to take into account the properties of the Cu and Cr films using a rule of mixtures approach and the following material constants: $E_{Cu} = 115$ GPa, $E_{Cr} = 279$ GPa, $\nu_{Cu} = 0.34$, $\nu_{Cr} = 0.21$. This technique has been utilized for brittle metal films [18,21,22] and multilayer films [35]. However, as will be described here, it can also be used to calculate the interfacial adhesion energy of thick (>100 nm) ductile films with the addition of the hard overlayer.

3. Results/discussion

Straining the two film systems in situ inside the SEM illustrated the ductility of the CuTi system and the brittle behavior of the CrCuTi system. The CuTi film was first observed to thin locally by forming necks at the yield strain at about 2.2% strain and then formed cracks at higher strains (Fig. 3a), while the CrCuTi system failed through brittle fracture at 0.7% strain (Fig. 3b). The cracking in both systems is through the film thickness of the whole multilayer and does not travel into the PI substrate.

Crack density (without necks) and surface deformation density (with necks) evolution of the CuTi film is shown in Fig. 4a from the in situ AFM experiment. The CuTi film can withstand almost 5% strain with minimal surface deformation. At strains below 5%, deformation was observed only in the form of necks in the AFM images as illustrated by the lack of through thickness cracks in Fig. 4a (black squares) below 5% strain. Further straining causes the initial necks to become through thickness cracks and they continue to emerge until saturation is reached at approximately 12% strain. At this strain no new surface deformation is observed, but necks could become through thickness cracks with even more strain. The average through thickness crack spacing is 6 ± 1.4 μm and the average surface deformation spacing is 4.2 ± 0.1 μm, both measured for the saturation regime between 12% and 15% strain. The surface deformation and crack spacings are most likely governed by the microstructure of the Cu film and the crack spacing of the underlying Ti film, however, more analysis is required before anything concrete can be reported. As shown in Fig. 4b, the cracks of the CrCuTi film initiate at a strain of about 0.7% and buckles form at approximately 7% strain. Also at the buckling strain, it was observed that the cracks reach the saturation region where no further cracks form and the average crack spacing is 13 ± 0.3 μm (determined for the saturation regime between 6% and 11% strain). The crack saturation region corresponded to a plateau in the film stress for both the Cr and Cu films with the in situ XRD straining to a maximum strain of 14% parallel to the straining

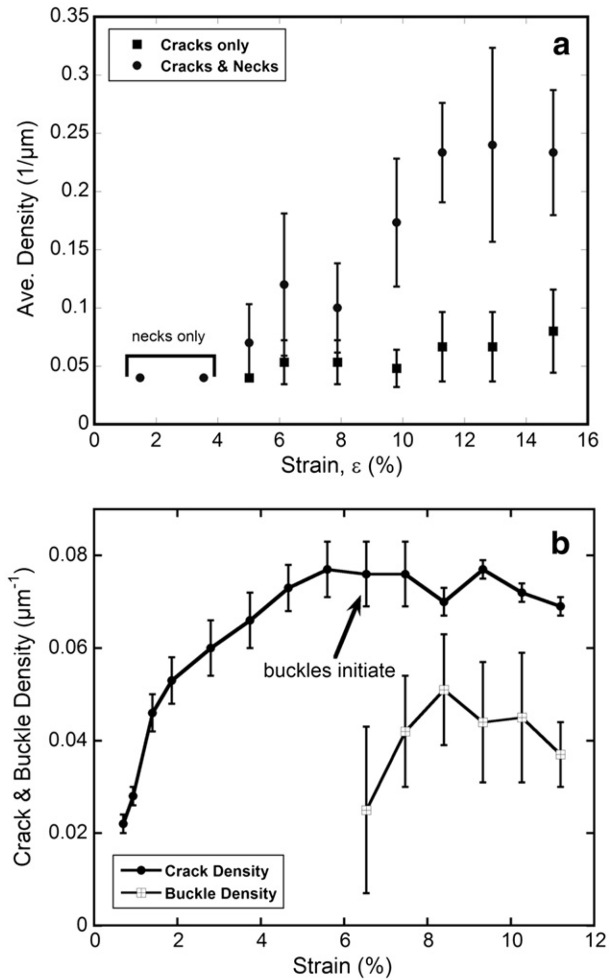

Fig. 4. (a) Crack density and surface deformation evolution of the CuTi as a function of the strain from the in situ AFM experiment. Cracks form after reaching 5% strain, while surface deformation in the form of necking occurs at much lower strains (b) Crack density evolution of the CrCuTi as a function of the strain from the in situ SEM experiment. Cracks initially formed at 0.7% strain and buckles at 7% strain.

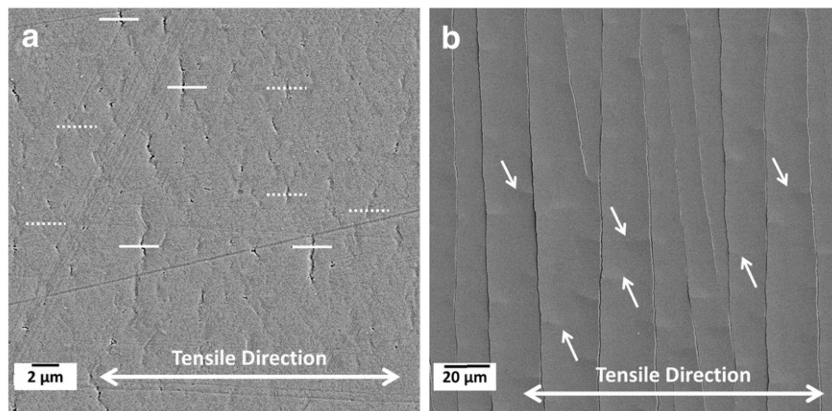

Fig. 3. SEM images of (a) CuTi film system strained to 16% with necks (dashed lines) and cracks (solid lines) indicated; (b) CrCuTi film system strained to 13% with partial buckles indicated with arrows.

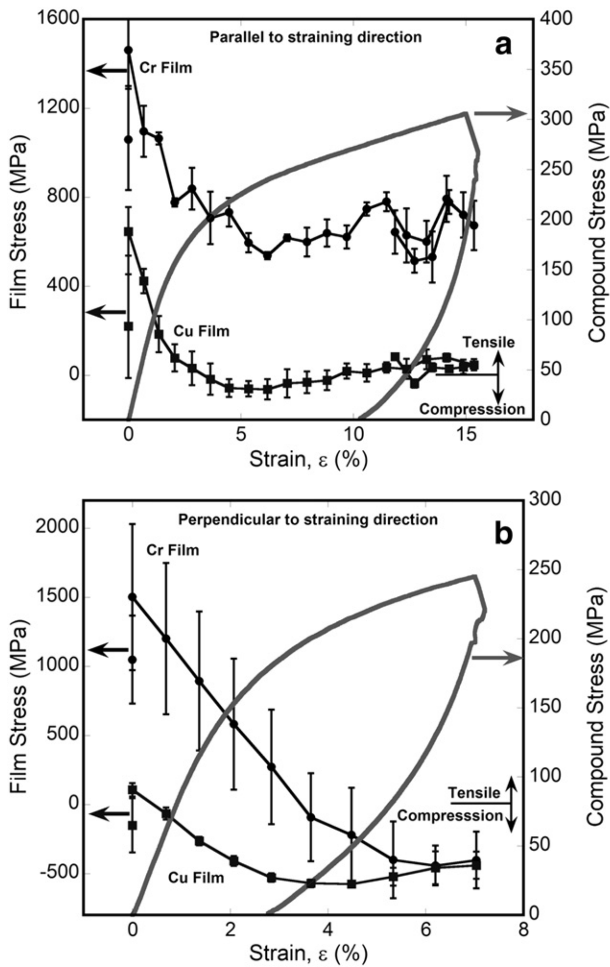

Fig. 5. (a) In situ straining with X-rays parallel to the straining direction. Both Cr and Cu film stresses reach a plateau at about 7% strain. (b) Stresses measured perpendicular to the straining direction of the Cr film start as tensile and decrease to compressive stresses correlating to delamination and buckle formation.

direction (Fig. 5a) and provides evidence that the crack saturation strain could be closely related to the buckling strain. At the plateau parallel to the straining direction, the stress in the Cr layer is 660 MPa (tensile) and the Cu layer is virtually stress-free. From the in situ SEM straining experiments, it was observed that the film will start to completely delaminate from the PI substrate at strains greater than 13%.

Because of the close correlation between the crack saturation strain and stress plateau, further stress measurements were made perpendicular to the straining direction of the CrCuTi sample. The results from the perpendicular straining (Fig. 5b) clearly indicate that the stress in the Cr film start as tensile and then decreases into the compressive regime. At the maximum prescribed strain, taken as the observed buckling strain from the in situ SEM experiment of 7%, both the Cr and Cu films are in a compressive state (-400 MPa). The transition into the compressive regime directly corresponds to the formation of buckles and the delamination of the Ti–PI interface.

With the buckles that formed on the CrCuTi samples the adhesion energy was calculated. The buckle heights and half buckle widths were measured from AFM images and input into the Cordill model for films on compliant substrates [14]. The ideal buckles to use with the adhesion model are those which have not traveled across the entire crack fragment. An example of such a buckle is shown in Fig. 6a and indicated in Fig. 3b. There are two main reasons that buckles of this type are better suited for the adhesion model. First, the shape of the buckle (Profile 2, Fig. 6b) is more rounded and the highest point of the buckle is not cracked (compared to Profile 1, Fig. 6b). The adhesion model is partially based on Euler buckling and the tent-shaped buckles (Profile 1) do not have the correct shape to fit the model. The second reason for the use of only the rounded buckles was due to the fact that the crack fragments themselves have a large amount of stress (660 MPa, tensile) and bend up at the edges (Fig. 7). Furthermore, Fig. 7 also illustrates how well the Cr overlayer aids in constraining the plastic deformation of the Cu film and a crack is forced to travel to the Ti–PI interface. This additional height would alter the adhesion measurement. The buckle dimensions were plotted as the $(\delta/h)^{1/2}$ versus (b/h) (Fig. 8). The data was then described by Eq. (1) with a fitting parameter, $\alpha = 7 \times 10^{-6}$. The α-parameter determines the adhesion of the interface through the relation (Eq. (2)).

Because the CuTi sample did not buckle, the adhesion energy could only be compared to that of a Ti–PI interface. It was found that the CrCuTi film buckle dimension lie between α values of 7×10^{-6} and 6×10^{-5} (Fig. 8). As discussed in Ref. [18], the minimum α value better describes the adhesion energy of the interface because the 2D model is only valid for buckles which have a symmetric cross-section and that no cracking of the film or substrate occurs during the buckling process. With this in mind, the measured adhesion of the CrCuTi sample was calculated to be 1 ± 0.3 J m^{-2}. Earlier work on the adhesion of a Ti–PI found that the adhesion energy of the interface to be 3.5 ± 1.2 J m^{-2} using the same technique and model [21]. The value for the CrCuTi film is lower compared to the single Ti layer and the difference could arise for several reasons. Recall that the CrCuTi crack fragments bend up at the edges due to the retained tensile stress after fracture and

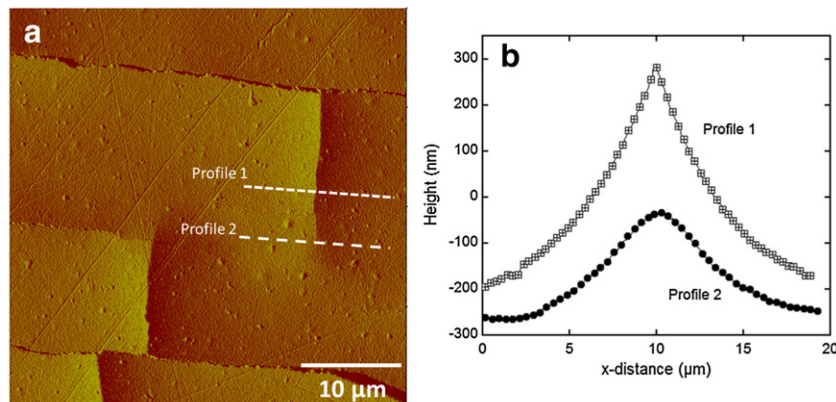

Fig. 6. (a) AFM deflection image of example buckles with two profiles (b) indicated.

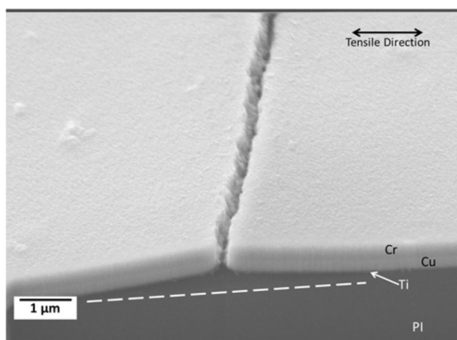

Fig. 7. FIB cross-section of CrCuTi film system illustrating that the crack fragments still contain tensile stress after fracture and bend up at the crack edges. It is also illustrated that the cracks travel through all three films and Ti–PI interface is the delaminating interface.

could be altering the buckling process with the additional shear stresses at the interface. Also, as pointed out by Toth et al. [34], the 2D model used is really only suitable to capture a lower bound adhesion energy and a 3D model is necessary to capture the buckling and delamination process properly with a case study. The application of the 3D model is currently underway. The calculated 1 J m^{-2} adhesion energy using the 2D model [18] is considered the lower bound and still compares very well with other metal–polymer systems and other adhesion models [12,16,18,21].

4. Conclusions

Measuring the adhesion of metal films on compliant polymer substrates requires the development of advanced techniques, especially for ductile films which deform plastically before the interface fails. The combination of a stressed overlayer and tensile straining can be used to induce cracking and delamination of the whole film system. In situ SEM, AFM and XRD straining revealed the through thickness cracking, delamination and the stress evolution in the films due to straining are all closely connected. Perpendicular to the straining direction, the stress in the Cr film system starts in a state of tension and with increased strain ends in a compressive state at the same stress buckles form. From the buckles the interfacial adhesion energy was calculated using the thermodynamic Cordill model [18] and measured to be 1 J m^{-2}. By including a stressed overlayer similar adhesion values were found between a single layer Ti–PI ($n = 3.5$ J m^2) interface and the multilayer (CrCuTi–PI) interface. The adhesion energy calculated here is also on the same order of a Au–PI interface [12] measured with four point bending and a Ta–PI interface measures with a two-dimensional shear lag model [16]. Both interfaces yielded an adhesion energy also of 1 J m^2. This study demonstrates that stressed overlayers, usually employed to delaminate films from rigid substrates could also be used on polymer substrates as well.

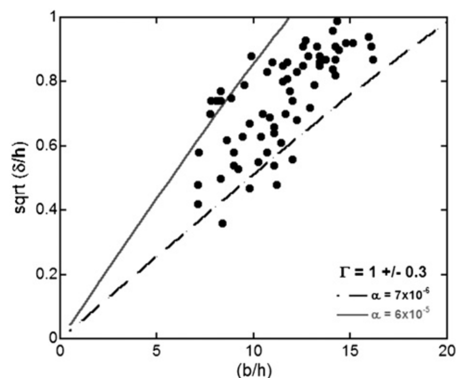

Fig. 8. Buckle measurements plotted using the Cordill model [18].

Acknowledgments

J. Schalko, P. Svasek and F. Kohl of the Institute for Integrated Sensor Systems, Austrian Academy of Sciences (Wiener Neustadt) are acknowledged for providing films used in this study. I. Zizak of the Helmholtz-Zentrum Berlin für Materialien und Energie GmbH is also gratefully acknowledged for beamtime assistance. Funding for this research has been provided by the Austrian Science Fund (FWF) under Project: P22648-N20 and by the Helmholtz-Zentrum Berlin (project nos. 2011_2_110211 and 2012_1_111115).

References

[1] J.A. Rogers, Z. Bao, K. Baldwin, A. Dodabalapur, B. Crone, V.R. Raju, V. Kuck, H. Katz, K. Amundson, J. Ewing, P. Drzaic, Paper-like electronic displays: Large-area rubber-stamped plastic sheets of electronics and microencapsulated electroniphoretic inks, PNSA 98 (2001) 4835.
[2] I. Graz, M. Kaltenbrunner, C. Keplinger, R. Schwoediauer, S. Bauer, S.P. Lacour, S. Wagner, Flexible ferroelectric field-effect transistor for large-area sensor skins and microphones, Appl. Phys. Lett. 89 (2006) 073501-1-3.
[3] C.J. Brabec, N.S. Sariciftic, J.C. Hummelen, Plastic Solar Cells, Adv. Funct. Mater. 11 (2001) 15.
[4] S.H. Ahn, L.J. Guo, High-speed roll-to-roll nanoimprint lithography on flexible plastic substrates, Adv. Mater. 20 (2008) 2044.
[5] F.C. Krebs, J. Fyenbo, M. Jorgensen, Product integration of compact roll-to-roll processed polymer solar cell modules: methods and manufacture using flexographic printing, slot-die coating and rotary screen printing, J. Mater. Chem. 20 (2010) 8994.
[6] Y. Xiang, T. Li, Z. Suo, J. Vlassak, High ductility of a metal film adherent on a polymer substrate, Appl. Phys. Lett. 87 (2005) 161910-1-3.
[7] T. Li, Z. Suo, Deformability of thin metal films on elastomer substrates, Int. J. Solids Struct. 43 (2006) 2351.
[8] M.D. Kriese, N.R. Moody, W.W. Gerberich, Quantitative adhesion measures of multilayer films: Part I. Indentation Mechanics, J. Mater. Res. 14 (1999) 3007.
[9] A.A. Volinsky, N.R. Moody, W.W. Gerberich, Interfacial toughness measurements for thin films on substrates, Acta Mater. 50 (2002) 441.
[10] M.J. Cordill, D.F. Bahr, N.R. Moody, W.W. Gerberich, Recent developments in thin film adhesion measurements, IEEE Trans. Device Mater. Reliab. 4 (2004) 163.
[11] A. Bagchi, A.G. Evans, Measurements of the debond energy for thin metallization lines on dielectrics, Thin Solid Films 286 (1996) 203.
[12] J.D. Yeager, D.J. Phillips, D.M. Rector, D.F. Bahr, Characterization of flexible ECoG electrode arrays for chronic recording in awake rats, J. Neurosci. Methods 173 (2008) 279.
[13] P.G. Charalambides, J. Lund, A.G. Evans, R.M. McMeeking, A test specimen for determining the fracture resistance of biomaterial interfaces, J. Appl. Mech. 56 (1989) 77.
[14] Y. Leterrier, J. Andersons, Y. Pitton, J.A.E. Mason, Adhesion of silicon oxide layers on poly (ethylene terephthalate). II. Effect of coating thickness on adhesive and cohesive strengths, J. Polym. Sci. B 35 (1997) 1463.
[15] Y. Leterrier, A. Mottet, N. Bouquet, D. Gillieron, P. Dumont, A. Pinyol, L. Lalande, J.H. Waller, J.A.E. Manson, Mechanical integrity of thin inorganic coatings on polymer substrates under quasi-static, thermal and fatigue loadings, TSF 519 (2010) 1729.
[16] S. Frank, U.A. Handge, S. Olliges, R. Spolenak, The relationship between thin film fragmentation and buckle formation: Synchrotron-based in-situ studies and two-dimensional stress analysis, Acta Mater. 57 (2009) 1442.
[17] J. Andersons, S. Tarasovs, Y. Leterrier, Evaluation of thin film adhesion to a compliant substrate by the analysis of progressive buckling in the fragmentation test, Thin Solid Films 517 (2009) 2007.
[18] M.J. Cordill, F.D. Fischer, F.G. Rammerstorfer, G. Dehm, Adhesion energies of Cr thin films on polyimide determined from buckling: Experiment and model, Acta Mater. 58 (2010) 5520.
[19] M.J. Cordill, K. Schmidegg, G. Dehm, Interface failure and adhesion measured by focused ion beam cutting of metal–polymer interfaces, Philos. Mag. Lett. 91 (2011) 530.
[20] M.J. Cordill, A. Taylor, J. Schalko, G. Dehm, Microstructure and adhesion of as-deposited and annealed Cu/Ti films on polyimide, Int. J. Mater. Res. 102 (2011) 729.
[21] A.A. Taylor, M.J. Cordill, L. Bowles, J. Schalko, G. Dehm, An elevated temperature study of a Ti adhesion layer on polyimide, Thin Solid Films 531 (2013) 354.
[22] O. Kraft, M. Hommel, E. Arzt, X-ray diffraction tool to study the mechanical behavior of thin films, Mater. Sci. Eng. A 88 (2000) 209.

[23] J. Lohmiller, N.C. Woo, R. Spolenak, Microstructure-property relationship in highly ductile Au–Cu thin films for flexible electronics, Mater. Sci. Eng. A 527 (2010) 7731.
[24] N. Lu, X. Wang, Z. Suo, J. Vlassak, Metal films on polymer substrates stretched beyond 50%, Appl. Phys. Lett. 91 (2007) 221909-1-3.
[25] M.J. Cordill, V.M. Marx, In-situ tensile straining of metal films on polymer substrates under an AFM, MRS Symposium Proceedings 1527, 2013, http://dx.doi.org/10.1557/opl.2013.617.
[26] I.C. Noyan, J.B. Cohen, Residual Stress: Measurement by Diffraction and Interpretation, Springer Verlag, New York, 1987.
[27] A. Erko, I. Packe, C. Hellwig, M. Fieber-Erdmann, O. Pawlizki, M. Veldkamp, W. Gudat, AIP Conf. Proc. 521 (2000) 415.
[28] L. Spieß, R. Schwarzer, H. Behnken, G. Teichert, Moderne Röntgenbeugung, B. G Teubner, Verlag, 2005.
[29] W.S. Rasband, Image J, U. S. National Institutes of Health, Bethesda, Maryland, USA http://rsbweb.nih.gov/ij/.
[30] M.J. Cordill, V.M. Marx, Fragmentation testing for ductile thin films on polymer substrates, Philos. Mag. Lett. 93 (2013) 618.
[31] P.O. Renault, P. Villain, C. Coupeau, P. Goudeau, K.F. Badawi, Damage mode tensile testing of thin gold films on polyimide substrates by X-ray diffraction and atomic force microscopy, Thin Solid Films 424 (2003) 267.
[32] G. Rochat, P. Fayet, Characterization of mechanical properties of ultra-thin oxide coatings on polymers by uniaxial fragmentation tests, J. Adhes. Sci. Technol. 26 (2012) 2381.
[33] H. Jin, W. Lu, M.J. Cordill, K. Schmidegg, In-situ study of cracking and buckling of chromium films on PET substrates, Exp. Mech. 51 (2011) 219.
[34] F. Toth, F.G. Rammerstorfer, M.J. Cordill, F.D. Fischer, Detailed modelling of delamination of buckling of thin films under global tension, Acta Mater. 61 (2013) 2425.
[35] K. Wu, J.Y. Zhang, G. Liu, P. Zhang, P.M. Cheng, J. Li, G.J. Zhang, J. Sun, Buckling behaviors and adhesion energy of nanostructured Cu/X (X = Nb, Zr) multilayer films on a compliant substrate, Acta Mater. 61 (2013) 7889.